

RSC Advances



This is an *Accepted Manuscript*, which has been through the Royal Society of Chemistry peer review process and has been accepted for publication.

Accepted Manuscripts are published online shortly after acceptance, before technical editing, formatting and proof reading. Using this free service, authors can make their results available to the community, in citable form, before we publish the edited article. This *Accepted Manuscript* will be replaced by the edited, formatted and paginated article as soon as this is available.

You can find more information about *Accepted Manuscripts* in the [Information for Authors](#).

Please note that technical editing may introduce minor changes to the text and/or graphics, which may alter content. The journal's standard [Terms & Conditions](#) and the [Ethical guidelines](#) still apply. In no event shall the Royal Society of Chemistry be held responsible for any errors or omissions in this *Accepted Manuscript* or any consequences arising from the use of any information it contains.

Fabrication and electrochemical characterization of Zn-Halloysite nanotubes composite coatings

S. Ranganatha, T.V. Venkatesha*

Department of studies in chemistry, School of chemical sciences, Kuvempu University, Shankaraghatta-577451, Shimoga, Karnataka, India.

* Corresponding author. Tel: +91-9448855079; fax: +91-08282-256255

E-mail addresses: drtvvenkatesha@yahoo.co.uk (Prof. T.V. Venkatesha)

kamath.ranganath@gmail.com (Dr. S. Ranganatha)

Abstract

The Zn-Halloysite nanotubes (HNT) composite coatings through electrodeposition technique were successfully fabricated on mild steel substrate. As a comparison pure zinc coating was also prepared. The composites were deposited in the presence of surfactants Cetyltrimmonium bromide (CTAB) and Sodium Lauryl sulfate (SLS). The effect of addition of nanoparticles and surfactants towards the deposition, crystal structure, texture, surface morphology and electrochemical corrosion behavior were studied. For characterization of the electrodeposits, the techniques such as X-ray diffraction (XRD), Scanning Electron Microscopy (SEM) coupled with Energy Dispersive X-ray analysis were made use. Both the additives HNTs and surfactants polarize the reduction process and thus influence the deposition process, surface nature and electrochemical properties. The electrochemical experiments like potentiodynamic polarization and Electrochemical Impedance Spectroscopy (EIS) studies carried out in 3.5% NaCl solution explicit higher corrosion resistance by HNT incorporated coating which was fabricated in the presence of CTAB. Microhardness of the deposits was evaluated and composite with higher incorporation of nanoparticles which was in the presence of CTAB exhibited highest value.

1 Introduction

Electrodeposition of zinc is a widely used industrial process to coat on steel materials to enhance its service life. Zinc being more active than iron, protects sacrificially by forming white rust. This white rust can be controlled by chromating the surface of zinc using chromic acid. But the effluent of this is hazardous to the environment and chromating process is avoided. To overcome this limitation some organic molecules were introduced as chelating agent and generated their thin film on zinc matrix with the idea of hindering interaction of corrosive medium with metal matrix¹. Increasing and demanding technological applications have led to the development of new coatings such as zinc alloy and/or zinc composite coatings. Metal/alloy coatings containing minute amounts of metal oxides, metal carbides, CNTs have been produced called composite coatings²⁻⁶. The recent investigations on composite zinc coatings revealed their higher corrosion resistance property, with higher wear resistance and microhardness⁷⁻⁹.

Halloysite nanotubes (HNTs) are a kind of naturally occurring aluminosilicate clay with a predominantly hollow nanotube structure and can be obtained from the natural environment. Halloysite is mainly composed of a two-layered aluminosilicate with the composition $\text{Al}_2\text{Si}_2\text{O}_5(\text{OH})_4 \cdot 2\text{H}_2\text{O}$, chemically similar to kaolinite, dickite or nacrite, differing mainly in the morphology of crystal. It is a layered clay mineral, consisting of one alumina octahedron sheet and one silica tetrahedron sheet in a 1:1 stoichiometric ratio. The length of HNTs varies in the range of 1–15 μm . HNTs have an inner diameter of 10–30 nm and an outer diameter of 50–70 nm, depending on the deposits. The chemical properties of the HNTs' outermost surface are similar to the properties of SiO_2 , while the properties of the inner cylinder core could be associated with those of Al_2O_3 ¹⁰.

Nanotubes with a hollow cavity have attracted a great deal of interest in both scientific and industrial fields. They possess novel physical and chemical properties derived from the structural versatility and provide opportunities for advanced applications in the fields of electronics, optics, catalysis, energy storage, and biological systems. Carbon nanotubes of different kinds are being used for numerous applications. HNTs resemble CNTs from their unique crystal structure and are readily obtainable. Some recent literature related to HNTs has shown the potential to provide cheap alternatives to expensive CNTs as they possess tubular structure in nano-scale¹⁰⁻¹¹.

The utility of HNTs is restricted to only some polymer composites which results in higher and enhanced mechanical properties like tensile strength, capacity to withstand force etc. As for as corrosion is concerned, interestingly these HNTs are utilized as nanocontainers for the corrosion inhibiting organic molecules with concern that of regulated release of inhibitor. These HNTs have been successfully used in the fabrication of electroless Ni-P-HNT composite coatings and showed improved properties corrosion resistance, friction resistance and microhardness¹¹. The success of a composite lies in the better reinforcement of the secondary materials into the matrix. The usage of surfactants of different structure and chemical nature to enhance the particle density in the coating and their effect on the process of electrodeposition has been reported previously⁷⁻⁸. This being the case, it will be of great deal of interest to study the HNT incorporated electrodeposits in presence of different surfactants which can bring about new properties to surfaces¹²⁻¹³.

In this regard, these halloysite nanotubes with 50 nm diameter and of several micrometers of length are utilized for the development of surfaces and studies on change in the surface properties have been successfully made in this. In this work,

HNTs are incorporated into growing zinc matrix. The effect of HNTs' inclusion is studied by SEM, EDX and XRD studies. The surfactants Cetyltrimmonium bromide (CTAB) and Sodium Lauryl sulfate (SLS) are used to improve the inclusion of the particles. The corrosion studies were made for the films through Tafel experiments and impedance spectroscopy. It is a novel composite material which can improve the corrosion stability in vigorous conditions.

2 Experimental

2.1 Materials

The composition of the plating bath for zinc and its composites is given in Table 1. The pH of bath solution was at 2.5 and it was adjusted by adding H₂SO₄. The halloysite nanotubes purchased from Sigma-Aldrich with product no. 685445 were used to fabricate the composite coatings. The agglomeration of nanotubes was minimized by subjecting the electrolyte to magnetic stirring for a period of 12h and ultrasonication prior to plating experiments.

The mild steel foils (AISI 1079 composition C = 0.5%, Mn = 0.5%, S = 0.005% and Fe = 98.95%) with dimensions of 40mm x 40mm x 1mm was used as cathode substrate. A pure zinc (99.99%) anode with 40mm x 40mm x 1mm dimensions was used for the deposition process. A potentiostat/galvanostat model PS-618 (Chemilink systems Mumbai) was used for the deposition of the coatings by DC currents. Throughout the composite deposition process the electrolyte was stirred at a speed of 300 rpm. After electrodeposition the samples were washed in distilled water for five minutes in order to remove the loosely adhered particles. Prior to plating experiments the mild steel plates (cathode) were polished to smooth surface using different grits of emery paper (600-4000) and degreased with trichloroethylene

followed by water wash and zinc (anode) surface was activated by dipping in 10% HCl for few seconds and was washed with water.

2.2 Characterization

2.2.1 Surface characterization

The surface morphology of coatings was investigated using JEOL-JEM-1200-EX II Scanning electron microscope. The particle content in the film was determined by energy dispersive X-ray analysis (EDX) coupled with SEM. X-ray diffraction (XRD) analysis of electrodeposits was carried out using a Philips TW 3710 X-ray diffractometer with Cu K α radiation ($\lambda=0.1540$ nm) working at 30 mA and 40 kV.

2.2.2 FTIR studies

Fourier transform infrared spectra (FT-IR) were obtained on KBr pellets at ambient temperature using a Bruker FT-IR spectrometer (TENSOR 27).

2.3 Electrochemical studies

2.3.1 Cathodic polarization studies (Deposition studies)

For cathodic polarization studies the working electrode was a disk of mild steel which was embedded in a Teflon holder and the area exposed was 0.13 cm². Prior to each experiment the mild steel electrode was first polished with different grits of emery paper (1200–4000) and then with alumina powders from 3 to 0.05 μ m until to get mirror finish. Cathodic scans were performed by ramping the potential from -0.4 V down to -1.4 V. The electrochemical measurements were performed using CHI660C electrochemical work station and all of them were carried out at a temperature of 25 ± 2 °C. A conventional single compartment glass of three electrode cell with 25 mL capacity, with a saturated calomel electrode as reference and a platinum wire as counter electrode was employed for measurements.

2.3.2 Corrosion studies

The potentiodynamic polarization and electrochemical impedance spectroscopy measurements were performed using a CHI660C electrochemical workstation. The measurements were performed using a conventional three-electrode cell, in which test sample was placed in Teflon sample holder and the exposed surface area to the corrosive medium was approximately 1cm^2 . The platinum wire serves as counter electrode and SCE electrode used as the reference electrode. Prior to the beginning of measurements the sample was immersed in the corrosive medium (3.5% sodium chloride, pH neutral) in order to establish the open circuit potential (E_{OCP}) or the steady state potential. The potentiodynamic polarization measurements were performed in non-deaerated conditions.

2.3.2.1 Tafel studies

The Tafel polarization study was used to calculate the kinetic parameters of the corrosion processes. The plots were obtained by varying the potential by $\pm 200\text{ mV}$ from the open circuit potential at a scan rate of 0.01 V/s in 3.5% NaCl.

2.3.2.2 Electrochemical Impedance Spectroscopic studies

The electrochemical impedance spectrum was recorded in the frequency range, of 10 mHz - 100 kHz , with data density of 6 points per decade. After each experiment the impedance data was displayed as Nyquist and Bode plots. The acquired data were curve fitted and analyzed using ZSimpWin 3.21 software.

2.4 Microhardness

The hardness of the coatings with the thickness of $15\mu\text{m}$ was measured using Knoop's indenter (Clemex microhardness tester, made in Japan). The time of application was 10 s with a load of 50g . The microhardness values quoted are an average of 5 measurements performed at different locations on each coating.

3 Results and discussion

3.1 Characterization of HNTs – FTIR, SEM & TEM

The halloysite nanotubes utilized for the preparation of composite coatings were purchased from Sigma-Aldrich (Product no. 685445). The SEM picture in the Fig. 1a shows the tubular structure of 1 – 3 μm long HNTs. As has been reported, HNTs contain two types of hydroxyl groups, inner and outer hydroxyl groups, which are situated between layers and on the surface of the nanotubes, respectively. Due to the multi-layer structure, most of the hydroxyl groups are inner groups and only a few hydroxyl groups are located on the surface of HNTs. The surface of HNTs is mainly composed of O–Si–O groups, and the siloxane surface can be confirmed from Fourier transform infrared spectrum Fig. 1b, in which a very strong absorption of O–Si–O at around 1020 cm^{-1} is observed. The 1094 cm^{-1} peak is assigned for stretching mode of apical Si-O. Two Al_2OH stretching absorptions at 3618 and 3695 cm^{-1} were noticed. Si-O bending absorbs at 462 cm^{-1} and a single bending Al-OH bending at 918 cm^{-1} . The band observed at 540 cm^{-1} is of deformation vibration of Al-O-Si. The absorption at 3441 cm^{-1} attributes O-H stretching of water and that of 1636 cm^{-1} O-H deformation of water. The peaks at 687 and 748 cm^{-1} are assigned for perpendicular Si-O stretching¹⁴⁻¹⁵.

3.2 Coating characterization

The Fig. 2a shows the surface morphology of the zinc electrodeposits of 15 μm thickness. The image C_0 shows zinc deposit without any additives. The C_C which is a HNT composite of zinc metal shows modified surface compared to the plain zinc. The HNT particles changed the morphology with smaller crystallites. The C_{CC} and C_{CS} represent the Zn-HNT composites in the presence of surfactants CTAB and SLS. It can be easily identified that, morphology of composite fabricated with CTAB is

severely modified compared to that of the composite prepared with SLS. The additives increase the nuclear number thereby creating competition between nucleation and crystal growth. During the electrodeposition process, metal ions from the electrolyte get reduced onto the surface of cathode. The additives which were carried along with the metal ions towards the cathode cover the reduced metal nuclei facilitating the formation of newer nuclear sites. This phenomenon prevents crystal growth on a particular metal seed which is the most beneficial to attain fine grained morphology, as it provides more number of nuclear sites preventing abrupt growth the deposit. In the case of CTAB, the development of a positive charge on the surface of particles is expected due to which more number of particles were drifted towards cathode leading to larger incorporation which ultimately results in finer grained crystal structure of the coating compared to other coatings. Further, the EDX results presented in next segment reflect the influence of surfactants on amount of particle reinforcement to the coating. Thus introduction of particles and surfactant molecules, result in smaller grain sizes. Fig. 2b shows the cross sectional SEM images of Zinc and Zinc composite. The C_{CC} clearly shows the incorporated particles in the presence of CTAB.

Coating composition has been evaluated by EDX technique. The Fig. 2c shows EDX spectra for Zn and Zn-HNT composite and Table 2 presents elemental composition of the deposits. Different kinds of surfactants are used and their effect on incorporation of particle into the metal matrix, reduction process and surface nature has been studied. For this purpose, a cationic surfactant CTAB and anionic SLS were used. The particular amount of surfactants were added to the electrolytic bath containing particles and given mechanical stirring. EDX analysis shows that the HNT incorporation is of around 3.7 wt.% in deposit C_C . But it varies with the

addition of surfactants. The CTAB increases its incorporation to 4.8 wt.% whereas SLS to 4.1 wt.%. The surfactants aid the ease of particle incorporation by facilitating the good dispersion in the electrolyte. However, the CTAB shows a higher performance in increasing the particle incorporation by creating a positive charge on the particle surface as it is a cationic surfactant. The possession of the positive charge makes the particles being attracted by cathode.

Fig. 3 displays the X-ray diffractograms and texture coefficients obtained for zinc deposits. It signifies the effect of surfactants and nanoparticles on crystallographic orientation and crystallinity of the deposits.

The determination of textures of the deposits is of so much interest as the electrocrystallization of zinc is very sensitive to bath composition. The preferred orientations of the deposits were determined using Muresan's method calculating the texture coefficients (Tc) with the equation [2]

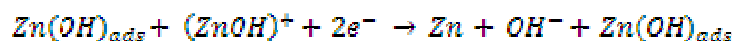
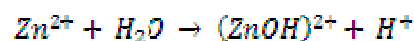
$$T_c = \frac{I_{(hkl)}}{\sum I_{(hkl)}} \times \frac{\sum I_0(hkl)}{I_0(hkl)}$$

where $I(hkl)$ is the peak intensity of the zinc deposits and $\sum I$ is the sum of intensities of the independent peaks. The index '0' refers to the intensity of standard zinc powder sample. The preferred crystallographic orientation is indicated by a Tc value larger than unity. The development of different crystal structures can be related to the surface energy differences which become driving force the relative growth of grain which have lowest surface energy and (0 0 2) plane is the lowest surface free energy owing to its compactness. The zinc coating except C_{CC} preferentially orients in (0 0 2) plane indicating effect of CTAB on crystal structure. Majority of Zn crystallites in pure zinc coating are oriented parallel to (1 1 0), (1 0 2) and (0 0 4) planes. Inclusion of the particles makes the zinc crystallites to orient along (0 0 2) and (0 0 4) to larger

extent. The surface morphologies of the deposits in the presence of surfactants have been modified, CTAB is strong enough to change the crystal structure in comparison with SLS. The most intense peak in the presence of CTAB is (1 0 1). The marked decrease in the basal (0 0 2) plane intensity is due to the modification of metal's surface energy by the adsorption of organic molecules. Increased surface energy can be held responsible for the deviation of hexagonal crystal structure with the addition of CTAB. The addition of particles and SLS has no much effect on the crystallographic orientation¹⁶⁻¹⁷.

3.3 Deposition studies - Cathodic polarization

Fig. 4 shows the cathodic polarization curves of the Zn-HNTs with and without surfactants. The deposition studies illustrate that HNTs cause an obstructive effect on the Zn^{2+} reduction. In the literature, it is reported that the metal Me^{2+} electrodeposition takes place in several steps. It is accepted that an intermediate Me^+ adsorption on the electrode during cathode reaction^{1,18}. During electroreduction, the localized concentration of hydroxide ions in close proximity to the cathode surface will increase and result in the formation of $MeOH_{ads}$. The probable chemical reaction path of zinc ions reduction is specified below¹⁹.



It is seen from the cathodic polarization curves that the addition of HNTs to the electrolyte causes the reduction potential of zinc to shift towards larger negatives,

but the slope of the reduction curve keeps unchanged. The shift to lower value in the reduction potential is attributed to a decrease in the active surface area of the cathode, owing to the adsorption of the particles, and may also relate to the decrease in the ionic transport by the HNTs, which does not significantly affect the electrochemical reaction mechanism. While comparing the effect of surfactants, CTAB as it is cationic surfactant directs higher number of particles towards the cathode compared to SLS which is an anionic one. Therefore, CTAB shifts the zinc deposition to higher negative values^{17, 20-21}.

3.4 Electrochemical studies

The Tafel polarization study was used to calculate the kinetic parameters of the corrosion process. The plots were obtained by varying the potential of deposits by ± 200 mV from the open circuit potential at a scan rate of 0.01 V/s using 3.5% NaCl at 25°C. The corrosion potentials (E_{corr}), corrosion rates (CR) and anodic/cathodic Tafel slopes (β_a and β_c) were obtained from the Tafel plots and are listed in Table 3. The polarization resistance values were determined using the relationship²²

$$I_{\text{corr}} = \frac{\beta}{R_p}$$

Where β is a constant calculated by the following equation

$$\beta = \frac{\beta_a \beta_c}{2.3 (\beta_a + \beta_c)}$$

where β_a and β_c (V^{-1}) are the Tafel slopes and R_p ($\Omega \text{ cm}^2$) is the polarization resistance and corrosion rates (CR) were calculated by the following equation

$$CR = \frac{0.13 I_{\text{corr}} \text{Eq. Wt.}}{d}$$

where Eq. wt. is the equivalent weight and d is the density (g/cm^3) of the zinc metal.

The Tafel plots were registered for various zinc coatings are shown in Fig. 5. It can be clearly noted that, R_p values are higher for composites compared to the plain zinc coating. The composite coatings deposited in the presence of surfactant CTAB shows highest R_p of $1001 \Omega \text{ cm}^2$ and least negative corrosion potential of -1.048 V thus highest corrosion resistance compared to that obtained in the presence of SLS.

The electrochemical impedance spectroscopic measurements were also employed to examine the chemical behavior of the zinc deposits. An equivalent circuit consisting of 2RC circuits shown in Fig. 6a was proposed. The two loops in the Nyquist diagram shown in Fig. 6b indicate that process consists of two relaxations or two time constants. All the curves are of same nature differing only in their point of intersection with Z_{real} axis which is being quantitative characteristic of corrosion resistance. The high frequency elements are related to the dielectric character C_{cot} of the coating that is reinforced by the ionic conduction through its pores (R_{cot}). Further, the low frequency contribution is attributed to the double layer capacitance (C_{dl}) at the coating electrolyte interface at the bottom of the pores coupled with the charge transfer resistance R_{ct} . Extent of chemical inertness for the selected corrosive medium can be analyzed through the resistance offered by the specimen, considering both coating and charge transfer resistance values. The bare zinc, C_0 possesses 110.9Ω . The introduction of particles to the zinc matrix makes to offer higher corrosion resistance by showing 178.7Ω . The presence of surfactants makes the composite more beneficial in terms of protection ability by enhancing the reinforcement. The higher corrosion resistance i.e., 534.4Ω in the presence of CTAB and 351.4Ω with SLS advocates the above discussion. The total resistance ($R=R_{\text{cot}} + R_{\text{ct}}$) increases with the addition of HNT particles into the growing zinc matrix. The Bode plots are displayed in Fig. 6c. The phase angle plot shows two humps which reflect the two

relaxation phenomena involved in the process. The impedance plot confirms highest impedance value for the deposit C_{CC} . Also, it is found that corrosion resistance is highest for the zinc composite deposited with CTAB. It can be advocated by the fact that, increased particle incorporation of the HNTs i.e., 4.8 wt.%, whereas the composite with SLS can only increase the particle incorporation up to 4.1 wt. %²³⁻²⁴. However, in the absence of surfactants the particle content was only 3.6 wt.% in the deposit C_C . Halloysite nanotubes have been used as the reinforcement to the growing zinc metal matrix. The resulting composite coating exhibited superior electrochemical properties. This enhanced property is a major contribution of the secondary material introduced to the metal coating. This can be pronounced by increasing the particles getting incorporated. Some factors govern the particle incorporation such as particle size and shape, relative density of the particles, inertness of the particles, concentration of the particles in plating bath, method and degree of adhesion, the orientation of the part being plated etc. Some methods like mechanical stirring/sonication and usage of surfactants enhance particle deagglomeration lead to increased incorporation. The types of second phase materials added to the coating are very much diverse consisting of different metal oxides, carbides and nitrides. These materials markedly improved the properties of bare zinc. CNTs from the carbonaceous family being very strong, highly chemically inert attracted the scientific community. But CNTs are very expensive and synthetic procedures are very tedious. The HNTs are very similar to CNTs in terms of structure. But these are very cheap, readily available naturally and superior to CNTs as they disperse better in solutions or polymer/metal matrices because they never intertwine each other unlike CNTs. This leads to significant properties by their composites^{1, 7, 16, 21-22}.

The SEM image shows that the deposit C_{CC} has the smaller grain size. The XRD results also support the above argument. Here, it should be noted that, particles distribution in the metal matrix plays crucial role and obviously uniform distribution will affect directly to the betterment in the surface properties. In this respect surfactant affect severely by adsorbing onto the particle surface. Particularly the CTAB, not only it adsorbs on the surface but also develops a positive surface charge which can further accelerate to incorporate on the cathode. Likewise, CTAB promotes even distribution of the particles in the composite compared to others. Further, as the particle content increases, the effective area exposed to the corrosive medium decreases also it may fill up any gaps, crevices or holes present in the growing metal matrix leading to compact and fine grained deposit.

3.5 Microhardness

The hardness values of the coated panels are shown in the Fig. 7. From the graph, it is observed that, the hardness value of the deposits with the introduction of HNTs. The composite coating possesses higher hardness compared to plain Zinc deposit. The deposits C_{CS} and C_{CC} are fine grained due to presence of the surfactants. Also, the included particles were found to be increased with the addition of surfactants. The composite prepared with CTAB exhibits highest hardness as it contains high number of included HNTs. During hardness measurements, the dispersed particles in the fine grained matrix may obstruct the easy dislocations; which was shown by higher hardness values of composite coatings fabricated in the presence of surfactants ²⁵.

5 Conclusion

The zinc and its HNT composite films were fabricated successfully. The incorporation of the particles was confirmed by EDX technique. The CTAB and SLS enhanced the incorporation of HNT in the deposit. The cathode polarization effect was appreciable in the presence of HNT and rendered the composite more corrosion resistance. Higher particle incorporation and fine grained crystal structure made Zn-HNT composite nobler than bare coating. Also, microhardness of the deposit was influenced greatly by amount of incorporated particles. The composite which was fabricated in the presence of CTAB was made successful to have incorporated high number of particles and shown highest hardness value.

Acknowledgement

The authors thank to Kuvempu University Karnataka, India for providing the lab facilities to bring about this work, and also CSIR, Govt. of India, for financial support by awarding Senior Research Fellowship (CSIR sanction no. 9/908(0003)2K12-EMR-I). Authors acknowledge Indian Institute of Science, Bangalore for extending some experimental facilities and Dr. Michael Rajamathi, Dept. of Chemistry, St. Joseph's College, Bangalore for providing XRD facility.

References

- [1] B.M. Praveen, T.V. Venkatesha, Y.A. Naik, and K. Prashantha, *Surf. Coat. Technol.*, 2007, **201**, 5836-5842.
- [2] S. Ranganatha, T.V.Venkatesha, K. Vathsala, M.K. Punith kumar, *Surf. Coat. Technol.*, 2012, **208**, 64-72.
- [3] S. Ranganatha , T.V. Venkatesha and K. Vathsala, *Mater. Res. Bull.*, 2012, **47**, 635-645.
- [4] S. Ranganatha, T.V. Venkatesha and K. Vathsala, *Ind. Eng. Chem. Res.*, 2012, **51** 7932-7940.
- [5] Ranganatha Sudhakar, Venkatarangaiah and T. Venkatesha, *Ind. Eng. Chem. Res.*, 2013, **52**, 6422-6429.
- [6] S. Ranganatha, T.V. Venkatesha, K. Vathsala, *Appl. Surf. Sci.*, 2010, **256**, 7377-7383.
- [7] B.M. Praveen and T.V. Venkatesha, *J. Alloys. Compd.* 2009, **482**, 53-57.
- [8] N. Boshkov, *Surf. Coat. Technol.*, 2003, **172**, 217-221.
- [9] Z.F. Lodhia, J.M.C. Mol, W.J. Hamer, H.A. Terryn and J.H.W. De Wit, *Electrochim. Acta*, 2007, **52**, 5444-5452.
- [10] Mingxian Liu, Baochun Guo, Mingliang Du, Xiaojia Cai and Demin Jia, *Nanotechnology* 2007, **18**, 455703
- [11] S. Ranganatha, T.V. Venkatesha and K. Vathsala, *Appl. Surf. Sci.*, 2012, **263** 149-156.
- [12] H. Ismail, Pooria Pasbakhsh, M.N. Ahmad Fauzi and A. Abu Bakar, *Polym. Test.* 2008, **27**, 841-850.
- [13] Youhong Tang , Shiqiang Deng , Lin Ye, Cheng Yang , Qiang Yuan, Jianing Zhang and Chengbi Zhao, *Composites: Part A*, 2011, **42**, 345-354.
- [14] Rayl Frost, *Clay. Clay. Miner.* 1995, **43**, 191-195.
- [15] Xiumei Sun, Yao Zhang, Hebai Shen and Nengqin Jia, *Electrochim. Acta.* 2010, **56**, 700-705.
- [16] A.Gomes and M.I.da Silva Pereira, *Electrochim. Acta.* 2006, **51**, 1342-1350.
- [17] R. Sen, S. Bhattacharya, S. Das and K. das, *J. Alloys Compd.* 2010, **489**, 650-656.
- [18] M. Rezrazi, M.L. Dochi, P. Bercot and J.Y. Hihn, *Surf. Coat. Technol.*, 2005, **192**, 124-130.

- [19] B.M. Praveen and T.V. Venkatesha, *Appl. Surf. Sci.*, 2008, **254**, 2418-2424.
- [20] K.O. Nayana and T.V. Venkatesha, *J. Electroanal. Chem.* 2011, **663**, 98-.
- [21] J. Fustes, A. Gomes and M.I. da Silva Pereira, *J. Solid State Electrochem.* 2008, **12**, 1435-1443.
- [22] K. Vathsala and T.V. Venkatesha, *J. Solid State Electrochem.*, 2012, **16**, 993-1001.
- [23] C Guo, Y Zuo, X Zhao, J Zhao and J Xiong, *Surf. Coat. Technol.* 2008, **202**, 3385-3390.
- [24] L. Shi, C.F. Sun, P. Gao, F. Zhou and W.M. Liu, *Surf. Coat. Technol.* 2006, **200**, 4870-4875.
- [25] B.M. Praveen and T.V. Venkatesha, *Appl. Surf. Sci.*, 2008, **254**, 2418-2424.

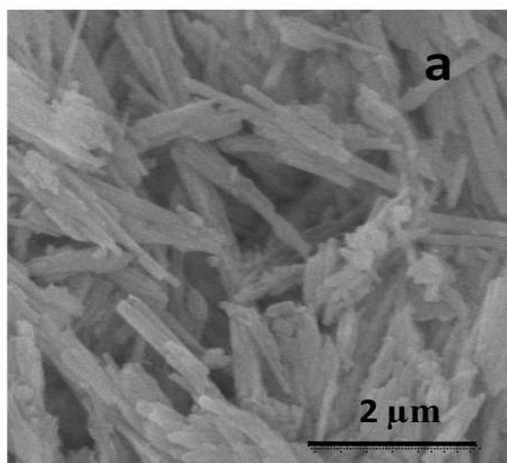


Fig. 1a. a) SEM picture of Halloysite nanotubes.

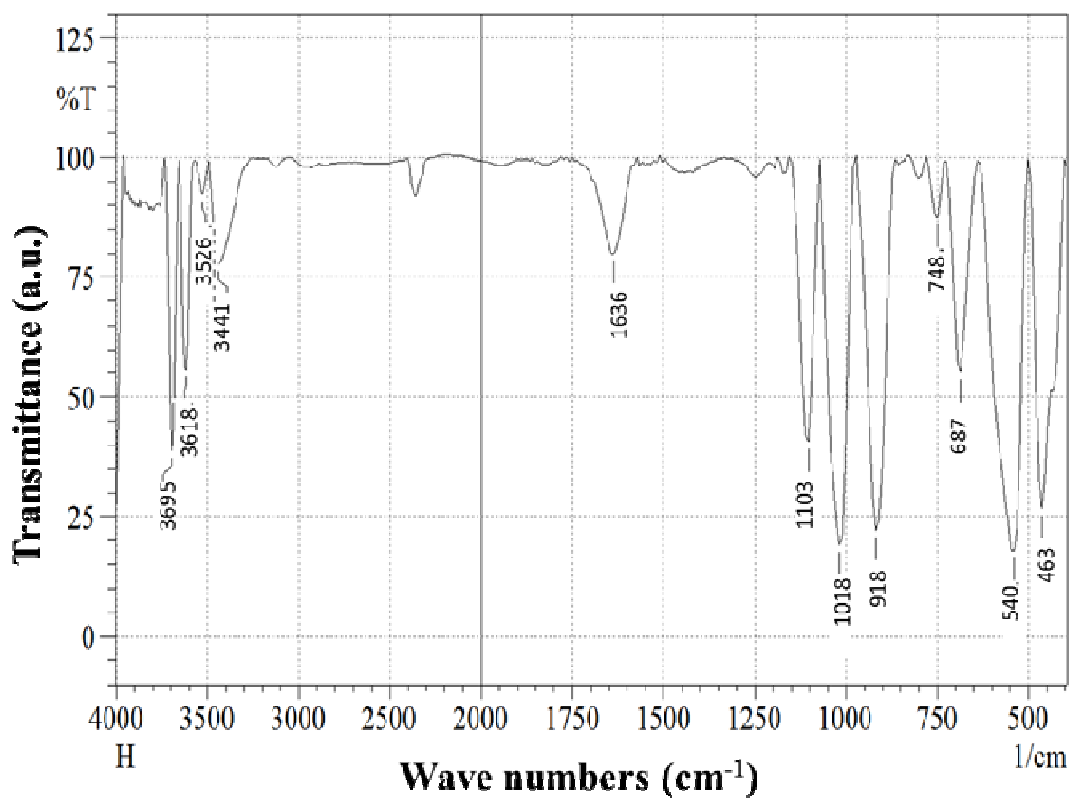


Fig. 1b. FTIR spectrum of HNT.

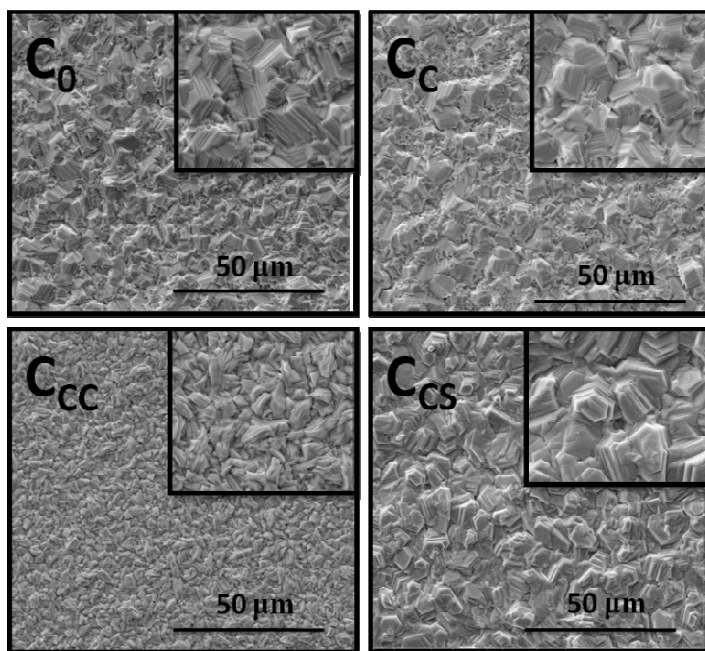


Fig. 2a. SEM images of the Zinc and Zinc composite coatings at different conditions.

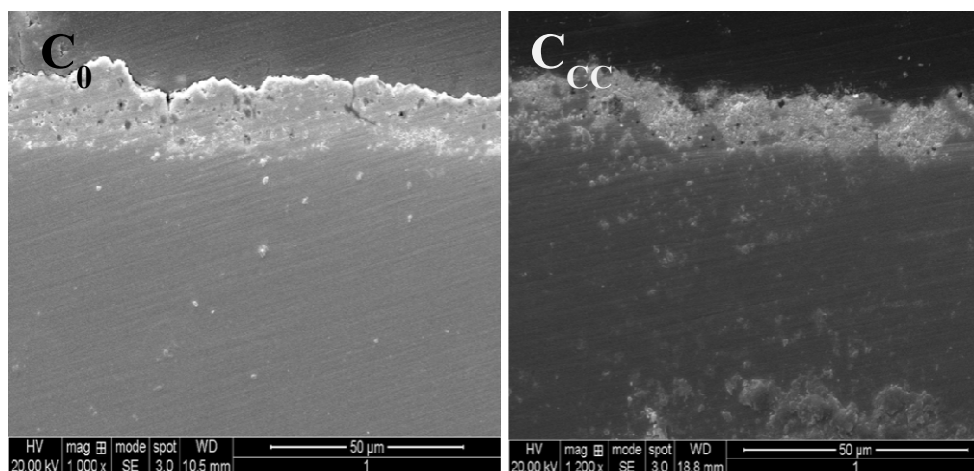


Fig. 2b. SEM cross sectional images of Zinc and Zinc-HNT composite.

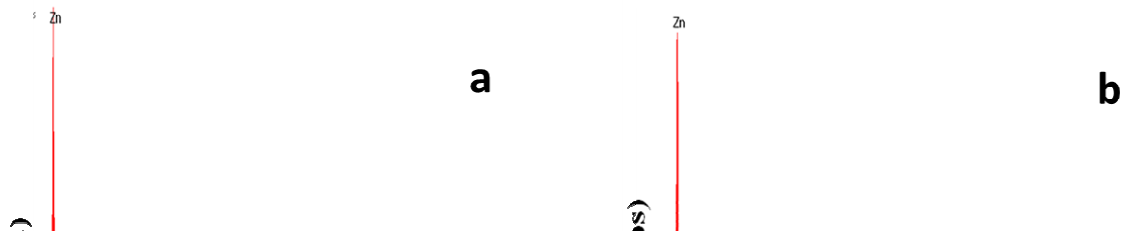


Fig. 2c. EDX spectra of a) Zinc and b) Zn-HNT composite coating.

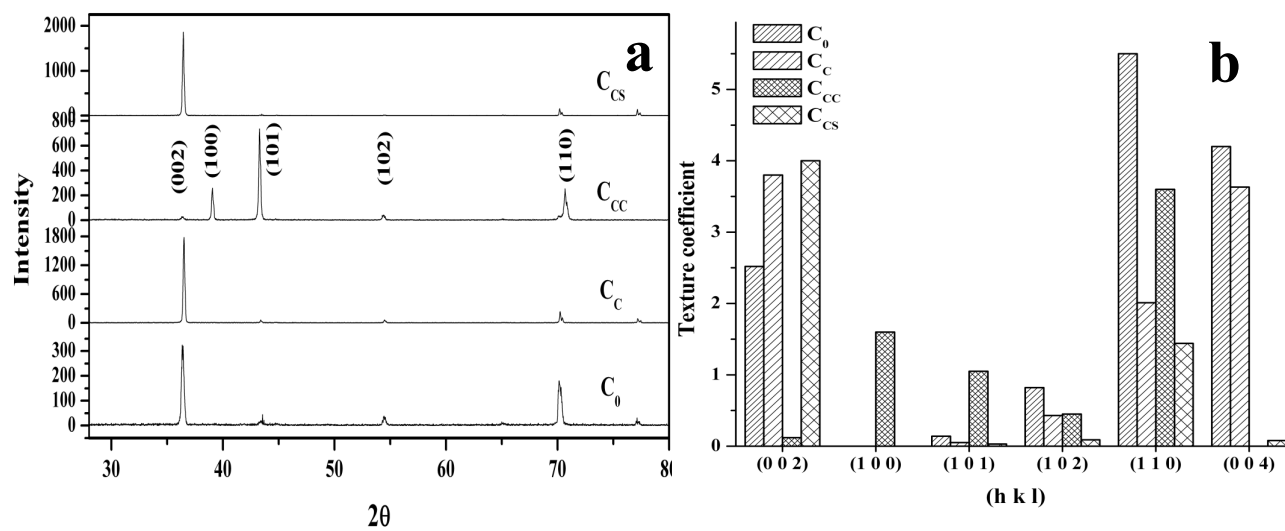


Fig. 3. a) XRD and **b)** Texture coefficients for the zinc deposits.

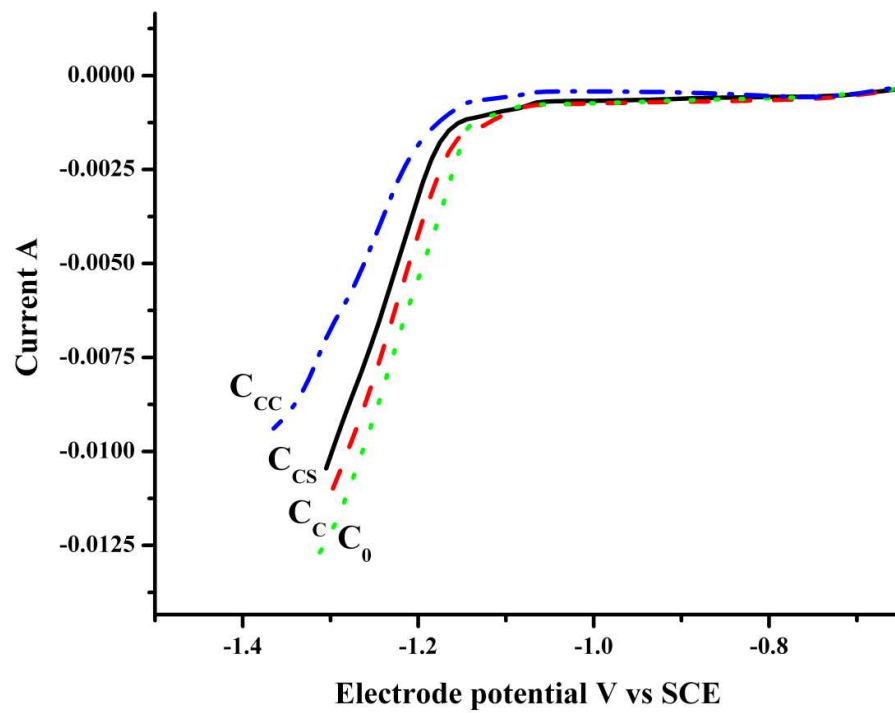


Fig. 4. Cathodic polarization curves for the composite bath solutions with and without surfactants.

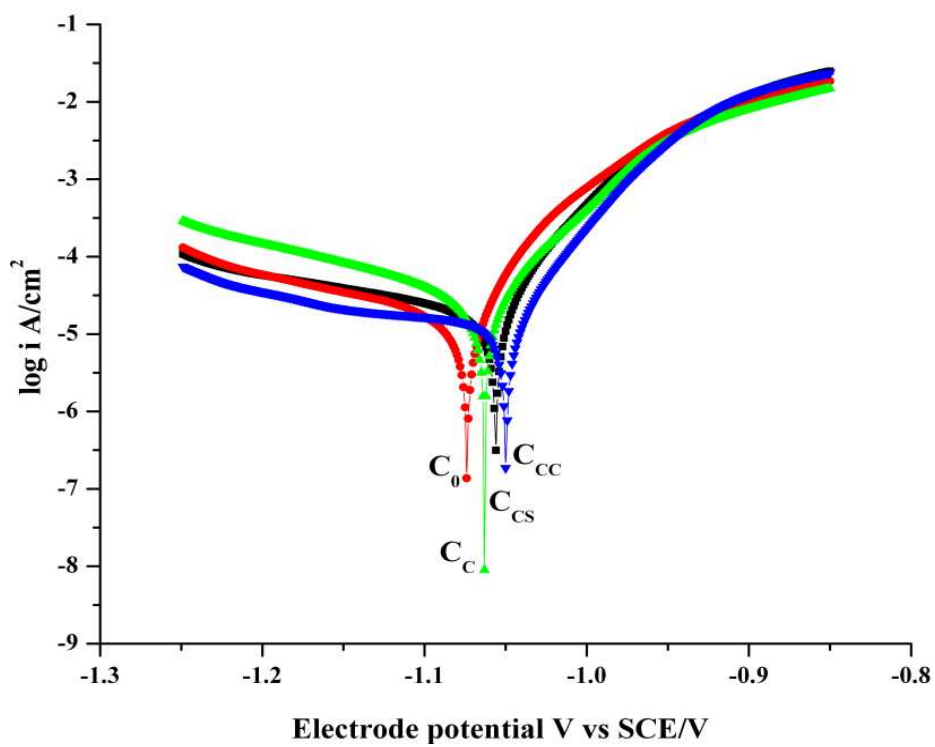


Fig. 5. Tafel curves for the zinc films in 3.5wt.% NaCl solution.

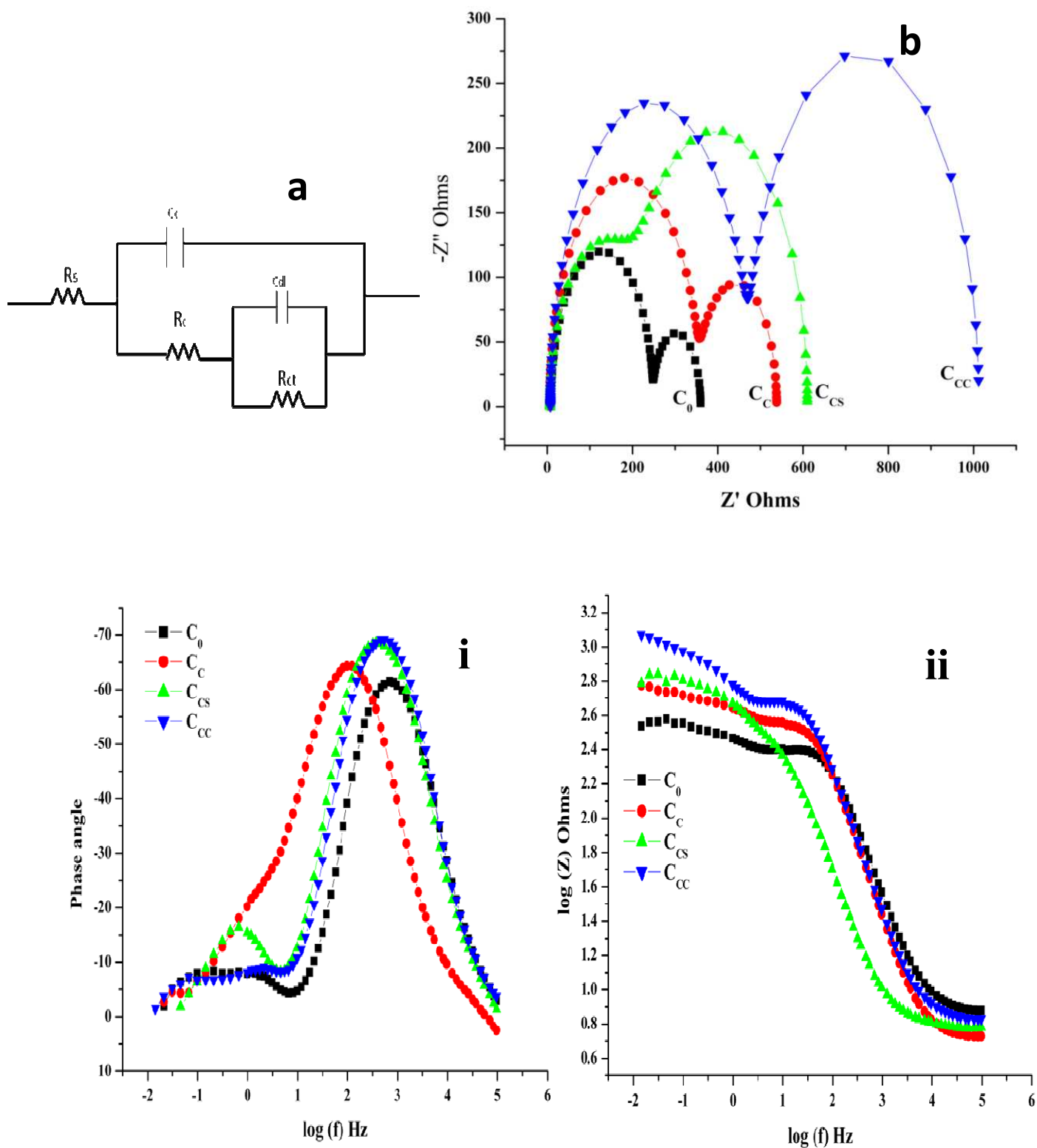


Fig. 6 a) Equivalent circuit, **b)** Nyquist plots for the zinc deposits in 3.5wt.% NaCl solution and **c)** Bode plots (i) Phase angle v/s frequency (ii) Impedance v/s frequency.

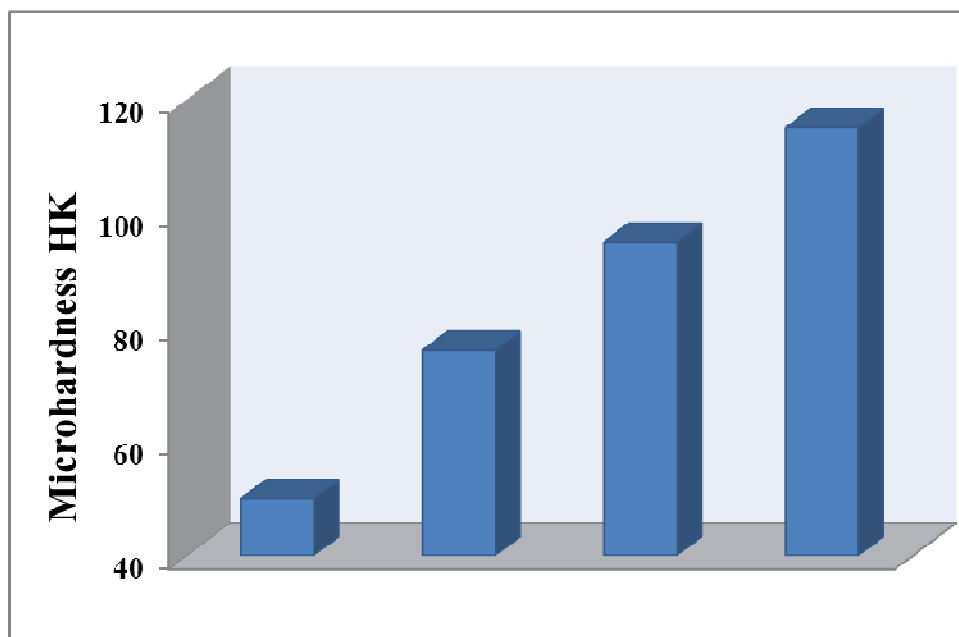


Fig. 7. Bar diagram showing microhardness values for various Zinc deposits.

Table 1 Composition of plating bath.

Bath composition	Bath parameters
ZnSO ₄ · 6H ₂ O – 200 g/L	pH – 2.5
Na ₂ SO ₄ – 30 g/L	Current density – 5 A/dm ²
NaCl – 10 g/L	Duration – 10 min
CTAB – 0.2 g/L	
SLS – 0.2 g/L	
HNT – 1 g/L	

Table 2 Elemental composition of the deposits obtained from EDX analysis.

Sample	Elemental composition in wt. %	
	Zn	HNT
C ₀	100	--
C _c	96.3	3.7
C _{cc}	95.2	4.8
C _{cs}	95.9	4.1

Table 3 Corrosion data for the zinc coatings from Tafel experiments.

Sample	E_{corr}	PR	I_{corr}	CR
	V	$\Omega \text{ cm}^2$	A cm^2	g/hr
C_0	-1.077	603	4.2×10^{-5}	8.7×10^{-5}
C_C	-1.061	679	3.2×10^{-5}	3.9×10^{-5}
C_{CC}	-1.048	1001	2×10^{-5}	2.7×10^{-5}
C_{CS}	-1.056	979	2.3×10^{-5}	2.8×10^{-5}

Table 4. Resistance values obtained from EIS experiments

Sample	$R = R_{\text{cot}} + R_{\text{ct}}$ $\Omega \text{ cm}^2$
C_0	111
C_C	179
C_{CS}	351
C_{CC}	534